ELSEVIER

www.elsevier.nl/locate/jorganchem

Journal of Organometallic Chemistry 589 (1999) 198–212

Journal of Organometallic Chemistry

Synthesis and molecular structure of hexaruthenium clusters containing unsaturated ring systems derived from 1-ethynylcyclopentanol, 1-ethynylcycloheptanol and 1-ethynylcyclooctanol

Cindy Sze-Wai Lau, Wing-Tak Wong *

Department of Chemistry, The University of Hong Kong, Pokfulam Road, Hong Kong, PR China

Received 28 April 1999

Abstract

Six hexaruthenium compounds which are identified as $[Ru_6C(CO)_{13}(\mu\text{-CO})\{\mu_3\text{-}\eta^1,\eta^2,\eta^3\text{-}C_5H_7CCC(H)C_5H_8\}]$ **1** (12%), $[Ru_6(CO)_{12}(\mu\text{-CO})_2\{\mu_4\text{-}\eta^1,\eta^1,\eta^2,\eta^4\text{-}CC(H)C_5H_6\}_2]$ **2** (8%), $[Ru_6C(CO)_{14}(\mu\text{-CO})\{\mu_2\text{-}\eta^1,\eta^3\text{-}C(H)C_7H_{11}\}]$ **3** (8%), $[Ru_6(CO)_{14}\{\mu_4\text{-}\eta^1,\eta^1\eta^2,\eta^4\text{-}CC(H)C_7H_{10}\}_2]$ **4** (10%), $[Ru_6C(CO)_{13}(\mu\text{-CO})\{\mu_3\text{-}\eta^1,\eta^2,\eta^3\text{-}C_8H_{12}C(H)C(H)C(H)C(OH)C_8H_{14}\}]$ **5** (16%), and $[Ru_6(CO)_{14}\{\mu_4\text{-}\eta^1,\eta^1\eta^2,\eta^4\text{-}CC(H)C_8H_{12}\}_2]$ **6** (8%) have been synthesised by reaction of $HC{\equiv}C(C_5H_8OH)$, $HC{\equiv}C(C_7H_{12}OH)$ and $HC{\equiv}C(C_8H_{14}OH)$, respectively, with triruthenium dodecacarbonyl in cyclohexane under refluxing conditions. All these compounds have been fully characterised by spectroscopic and X-ray diffraction methods. The structures of **1**, **3** and **5** are based on a Ru_6 octahedral skeleton containing a μ_6-carbide. Both clusters **1** and **5** involve the coupling of two functionalized alkyne molecules to give an unusual hexatetraene chain with the elimination of water molecules. Complex **3** consists of one alkyne moiety bonded to a Ru_3 triangular face via one σ and a π-allyl bond. An interesting feature in clusters **2**, **4** and **6** is the formation of a metallacyclic five-membered ring with a $\mu_4\text{-}\eta^1,\eta^1,\eta^2,\eta^4$ mode, which is derived from the C≡C triple bond and C–H bond activations. Reaction of $[Ru_3(CO)_{10}(NCMe)_2]$ with 1-ethynylcyclopentanol affords another new cluster, $[Ru_3(CO)_9(\mu\text{-CO})(\mu_3\text{-}\eta^1,\eta^1,\eta^2\text{-}HCCC_5H_8OH)]$ **7**, which consists of an alkyne ligand bound to the triruthenium cluster unit via a typical $\mu_3\text{-}(\eta^2\text{-}||)$ coordination mode.

Keywords: Ruthenium; Carbonyl; Clusters; Alkynes; Carbides

1. Introduction

The study of the synthesis and reactivity of transition metal carbonyl clusters with functionalised alkyne molecules has received considerable attention in recent years [1–8]. In our research work we have been particularly interested in the reaction of a triruthenium cluster with the hydroxy alkyne derivatives, but-3-yn-2-ol and 9-ethynyl-9-fluorenol. A prominent circumstance in these reactions is the formation of a range of new products involving extensive rearrangement of ligands, namely, dehydration and hydrogen atom transfer [9,10]. With the related unsaturated organic rings, two main distinctions may be used to classify the bonding type. First, π-bonded systems in which the ring bonds to one, two or three metal centres solely through the π electrons [11], and secondly σ systems in which one or more C–H bonds undergo cleavage with the formation of metal–carbon σ bonds [12]. These latter systems are often in association with π bonds but not generally through the entire π system. The synthesis of compounds of both types is important in improving our understanding of the chemisorption of molecules on metal surfaces [13], and the effect such bonding modes have on the reactivity of the organic molecules. Johnson and co-workers have recently published a series of papers related to ruthenium clusters containing cyclopentadiene, cycloheptatriene and cycloocta-1,3-diene ring systems, which show a wide range of bonding characteristics [14–16]. In this paper we report the results of the thermolytic reaction of $[Ru_3CO)_{12}]$ with

* Corresponding author. Fax: +852-25472933.
E-mail address: wtwong@hkucc.hku.hk (W.-T. Wong)

0022-328X/99/$ - see front matter
PII: S0022-328X(99)00403-9

1-ethynylcyclopentanol, 1-ethynylcycloheptanol and 1-ethynylcyclooctanol, bearing a saturated C_5, C_7 and C_8 ring, respectively. The saturated ring functionality was selected because of its potential to form additional π bonds, which appear to be capable of binding to the clusters. Other unusual transformations such as metallacycle formation [17] and ligand coupling are also observed [18]. Furthermore, an uncommon C≡C bond cleavage was noted during cluster build up likely to lead to carbido–hexaruthenium clusters [19]. The mechanism of this bond cleavage has not been fully elucidated.

2. Results and discussion

The reaction of $[Ru_3(CO)_{12}]$ with HC≡CR, where $R = C_5H_8OH$, $C_7H_{12}OH$ and $C_8H_{14}OH$, in refluxing cyclohexane (80°C) in a dinitrogen atmosphere generated two new products of each kind of ligands in relatively low yields, which in each case can be separated by preparative thin-layer chromatography (TLC) (Scheme 1). Altogether, six hexaruthenium compounds can be isolated and identified as $[Ru_6C(CO)_{13}(\mu\text{-}CO)\{\mu_3\text{-}\eta^1,\eta^2,\eta^3\text{-}C_5H_7CCC(H)C_5H_8\}]$ **1**, $[Ru_6(CO)_{12}(\mu\text{-}CO)_2\{\mu_4\text{-}\eta^1,\eta^1,\eta^2,\eta^4\text{-}CC(H)C_5H_6\}_2]$ **2**, $[Ru_6C(CO)_{14}(\mu\text{-}CO)\{\mu_2\text{-}\eta^1,\eta^3\text{-}C(H)C_7H_{11}\}]$ **3**, $[Ru_6(CO)_{14}\{\mu_4\text{-}\eta^1,\eta^1\text{-}\eta^2,\eta^4\text{-}CC(H)C_7H_{10}\}_2]$ **4**, $[Ru_6C(CO)_{13}(\mu\text{-}CO)\{\mu_3\text{-}\eta^1,\eta^2,\text{-}\eta^3\text{-}C_8H_{12}C(H)C(H)C(H)C(OH)C_8H_{14}\}]$ **5**, and $[Ru_6(CO)_{14}\{\mu_4\text{-}\eta^1,\eta^1\eta^2,\eta^4\text{-}CC(H)C_8H_{12}\}_2]$ **6**, in 12, 8, 8, 10, 16 and 8% yields, respectively [based on $Ru_3(CO)_{12}$]. Reaction of $[Ru_3(CO)_{10}(NCMe)_2]$ with 1-ethynylcyclopentanol affords the triruthenium cluster $[Ru_3(CO)_9(\mu\text{-}CO)(\mu_3\text{-}\eta^1,\eta^1,\eta^2\text{-}HCCC_5H_8OH)]$ **7** (20% yield). All the compounds were fully characterised by FAB mass spectrometry, IR and ^{1}H-NMR spectroscopies and single-crystal X-ray crystallography. The structure of compound **5** was also revealed by advanced NMR techniques.

2.1. Treatment of $[Ru_3(CO)_{12}]$ with 1-ethynylcyclopentanol

The first product was isolated as a brown band and its positive FAB mass spectrum displays a parent

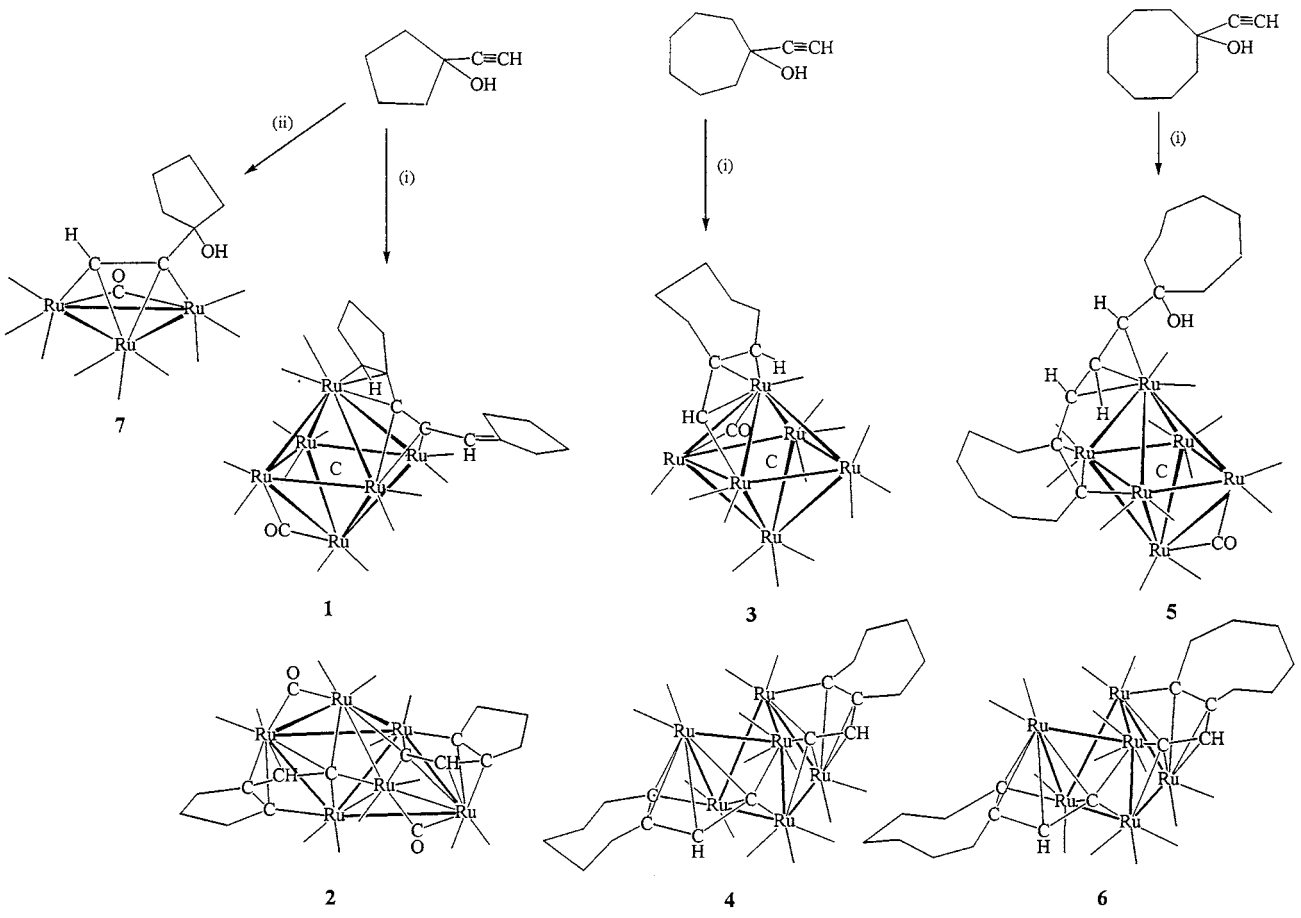

Scheme 1.

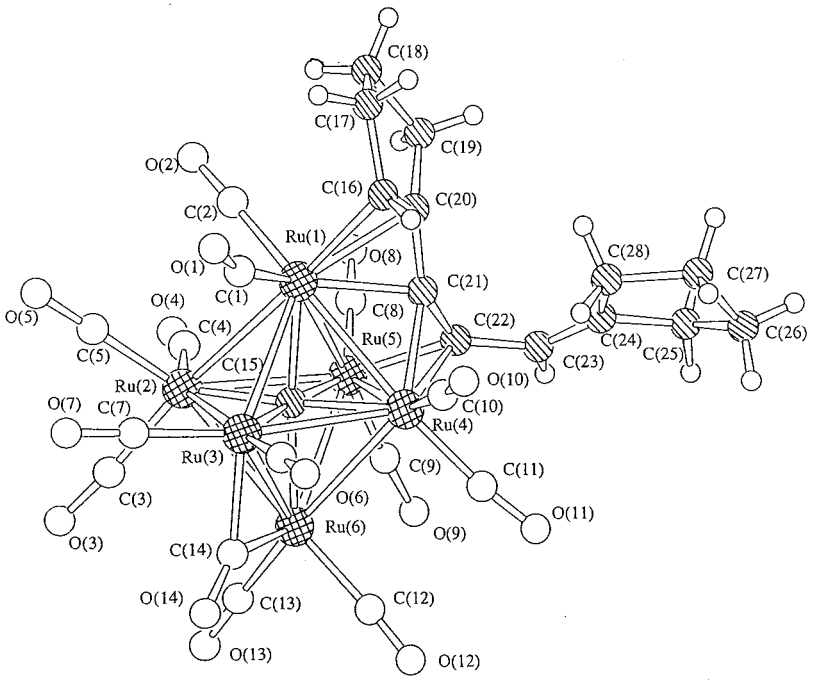

Fig. 1. Molecular structure of cluster **1**.

molecular ion peak at m/z 1183, as well as peaks corresponding to the sequential loss of carbonyl ligands (see Table 8). The ^{1}H-NMR spectrum in $CDCl_3$ shows a signal centred at δ 5.61 due to the methine proton on C(16) appearing as a quartet due to overlap of the two triplets with J(HH) 5.8 Hz, which is coupled to the non-equivalent methylene protons on C(17). A slightly downfield singlet signal appear at δ 3.66 for a proton on C(23). Also, a rather complex multiplet due to the 14 methylene protons of the two cyclopentyl rings was observed in the range δ 1.86–3.58. A single-crystal X-ray analysis was carried out on a brown crystal grown from an ethanol–*n*-hexane solution at -10°C. The asymmetric unit consists of two independent but structurally similar molecules of **1** and solvates of EtOH. A perspective drawing of cluster **1** with the atomic numbering scheme is shown in Fig. 1. Selected interatomic bonds and angles are shown in Table 1. The metal core of **1** comprises an octahedron encapsulating a carbido atom. The Ru–Ru bond distances range from 2.746(2) to 2.998(2) Å, while the Ru–C(carbide) bond distances are 1.96(2)–2.09(2) Å. These values are typical of those observed in other Ru_6C compounds [20]. A total of 13 carbonyl ligands in **1** are terminally bound to the Ru atoms, and the [C(14)–O(14)] is found to bridge Ru(3)–Ru(6), which is consistent with the band at 1845 cm^{-1} observed in the IR spectrum. The origin of the carbide atom in the carbido–transition metal carbonyl clusters has been the subject of some conjecture [21–23]. According to the number of dimerized alkyne carbons, it is possible that the carbido atom originates from the alkyne carbon via the cleavage of C≡C triple bond. It is well documented that the coordinated CO is an alternative source of carbide in transition metal cluster chemistry. However, it is worthy to note that a higher temperature is usually required for the reaction. For instance, heating of $Ru_3(CO)_{12}$ in cyclohexane or benzene at 150°C under nitrogen leads to $[Ru_6C(CO)_{17}]$ [24] and reaction of $Ru_3(CO)_{12}$ in toluene under reflux (110°C) for several days gives toluene-substituted derivatives of $[Ru_6C(CO)_{14}(C_6H_5CH_3)]$ [25]. In **1** the two functionalized alkyne units are coupled to yield an unusual 1,2,3,5-hexatetraene chain with the loss of two water molecules. The resulting ligand straddles the Ru(1)–Ru(4)–Ru(5) triangular face of the cluster **1** interacting via a novel μ_3-η^1,η^2,η^3 bonding mode. The C(16)–C(20)–C(21)–C(22) is probably best described as a rare butatrienylidene ligand [26] bonded to Ru(1), Ru(4) and Ru(5) atoms, in which the distances of the three C–C bonds, C(16)–C(20), C(20)–C(21), C(21)–C(22), are 1.43(2), 1.40(2) and 1.41(2) Å, respectively, indicating a double-bond character, while the C(16)–C(20)–C(21) angle is 118(1)° characteristic of sp^2 hybridisation. The C(16)–C(20)–C(21) fragment gives a η^3-allyl group coordinated to the Ru(1) based upon both C–C and C–H bond activations. The other C(21)–C(22) moiety forms a π-interaction to Ru(5) via a typical C≡C triple bond scission. The carbon C(22) atom also exhibits a strong σ bond to Ru(4)

[Ru(4)–C(22) 2.06(2) Å]. The second alkyne fragment coupled to the previous one forms a single bond C(22)–C(23), 1.50(2) Å, involving the cleavage of C≡C triple bond and C–H activation. It should be noted that the carbon atom C(24) exhibits a considerable amount of sp^2 character following the loss of the hydroxyl group to give a short C–C bond, C(23)–C(24) 1.29(3) Å. Two cyclopentyl rings are observed to skew so as to avoid the unfavourable clash between the protons located on C(19) and C(28). In this coordination mode, the resulting ligand acts as a six-electron donor, donating three electrons through η^3-allyl bonding to Ru(1), one electron through σ bond to Ru(4) and two electrons through the π-interaction to Ru(5). The total electron count for the cluster **1** is 86 and is electron-precise according to the PSEPT rule.

The chromatographic separation of the reaction mixture yielded the second fraction, which gave brown crystals of **2** after recrystallisation. Five multiplets centred at δ 2.81, δ 2.52, δ 2.22, δ 2.12 and δ 1.90 in the ratio of 1:2:1:1:1, respectively, may be assigned as the 12 methylene protons as shown in the ^{1}H-NMR spectrum (see Table 8). A considerably downfield singlet resonance at δ 5.30 corresponds to the two acetylenic protons on C(9 and 9*). The positive FAB mass spectrum exhibits a molecular ion peak at m/z 1181. A perspective drawing of cluster **2** with the atomic numbering scheme is shown in Fig. 2 and some relevant bond parameters are collected in Table 2. The molecule of **2** possesses exact C_2 symmetry. Its metal core consists of a distorted trigonal prism with an additional bond across the diagonal of one of the square faces [Ru(1), Ru(1*)]. Each ruthenium atom carries two terminal carbonyl ligands, and two bridging CO ligands are bound to Ru(2 and 2*) and Ru (3 and 3*), which is consistent with the band at 1835 cm^{-1} observed in the IR spectrum. The two alkynyl ligands with an unusual μ_4-η^1,η^1,η^2,η^4 bonding mode were coordinated to the metal core on the opposite side in order to minimise steric repulsion. Two acetylenic carbon atoms C(8 and 8*) are quadruply σ bridged across two distorted square planes and they also π interact with the Ru(3 and 3*), atom together with C(9 and 9*), respectively, via a C≡C triple bond activation. The four carbon atoms C(8), C(9), C(10) and C(11) are bonded to Ru(3) in a π-bonding mode, and additionally C(8) bridges the distorted square face Ru(1)–Ru(2)–Ru(3)–Ru(4) and C(11) forms a σ-bond to Ru(1). In the formation of these bonds, two hydrogen atoms have been lost from C(11) and the hydroxyl group from C(10). The overall metal–ligand bonding may be regarded as a ruthenacyclopentadiene ring (planar to within 0.16 Å] π bonded to Ru(3). Cluster **2** has 88 cluster valence electrons (CVEs) which obeys the EAN rule for the Ru_6 core with 10 metal–metal bonds.

Table 1
Some selected bond lengths (Å) and angles (°) for cluster **1**

Bond lengths (Å)			
Ru(1)–Ru(2)	2.917(2) [2.911(2)]	Ru(1)–Ru(3)	2.956(2) [3.023(2)]
Ru(1)–Ru(4)	2.779(2) [2.776(2)]	Ru(1)–Ru(5)	2.896(2) [2.871(2)]
Ru(2)–Ru(3)	2.894(2) [2.879(2)]	Ru(2)–Ru(5)	2.915(2) [2.994(2)]
Ru(2)–Ru(6)	2.970(2) [2.981(2)]	Ru(3)–Ru(4)	2.990(2) [2.910(2)]
Ru(3)–Ru(6)	2.806(2) [2.801(2)]	Ru(4)–Ru(5)	2.746(2) [2.766(2)]
Ru(4)–Ru(6)	2.998(2) [2.922(2)]	Ru(5)–Ru(6)	2.920(2) [2.996(2)]
Ru(1)–C(15)	2.06(2) [2.09(2)]	Ru(1)–C(16)	2.32(2) [2.30(2)]
Ru(1)–C(20)	2.29(2) [2.23(2)]	Ru(1)–C(21)	2.20(2) [2.21(2)]
Ru(2)–C(15)	1.96(1) [1.98(2)]	Ru(3)–C(14)	2.04(2) [2.08(2)]
Ru(3)–C(15)	2.07(2) [2.08(2)]	Ru(4)–C(15)	2.09(1) [2.06(2)]
Ru(4)–C(22)	2.29(2) [2.30(2)]	Ru(5)–C(15)	2.04(2) [2.04(2)]
Ru(5)–C(22)	2.06(2) [2.02(2)]	Ru(6)–C(14)	2.08(2) [2.03(2)]
Ru(6)–C(15)	2.08(2) [2.07(2)]	C(16)–C(17)	1.52(2) [1.55(2)]
C(16)–C(20)	1.43(2) [1.33(2)]	C(17)–C(18)	1.54(3) [1.52(3)]
C(18)–C(19)	1.58(3) [1.48(3)]	C(19)–C(20)	1.48(2) [1.55(2)]
C(20)–C(21)	1.40(2) [1.41(2)]	C(21)–C(22)	1.41(2) [1.34(2)]
C(22)–C(23)	1.50(2) [1.51(2)]	C(23)–C(24)	1.29(3) [1.36(2)]
C(24)–C(25)	1.53(3) [1.52(2)]	C(24)–C(28)	1.47(3) [1.53(2)]
C(25)–C(26)	1.52(3) [1.43(3)]	C(26)–C(27)	1.54(3) [1.51(3)]
C(27)–C(28)	1.55(3) [1.53(3)]		
Bond angles (°)			
Ru(2)–Ru(1)–Ru(3)	59.0(5) [58.7(2)]	Ru(1)–Ru(2)–Ru(3)	61.2(5) [62.9(5)]
C(20)–C(21)–C(22)	142(1) [143(1)]	C(16)–C(20)–C(21)	118(1) [121(1)]
C(22)–C(23)–C(24)	123(1) [122(1)]	C(21)–C(22)–C(23)	132(1) [136(1)]

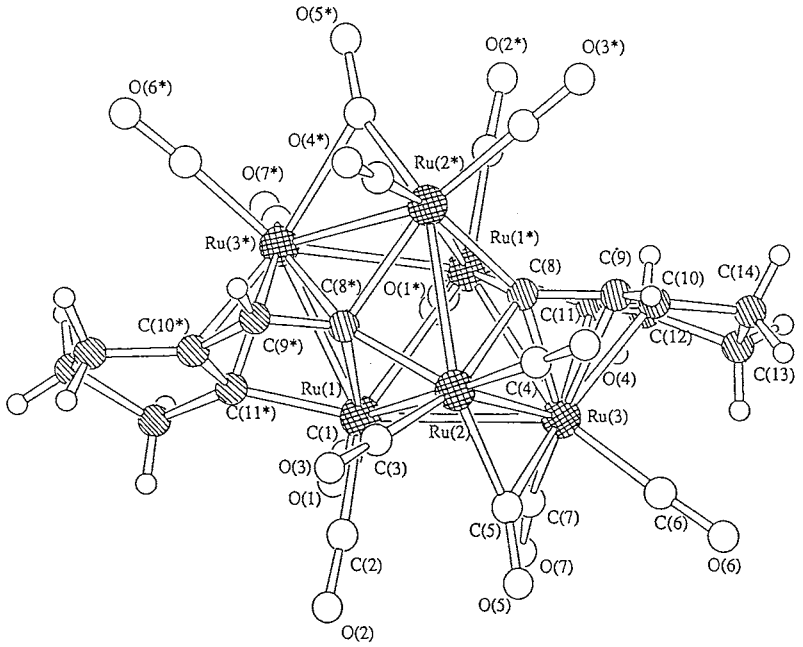

Fig. 2. Molecular structure of cluster **2**.

2.2. Treatment of $[Ru_3(CO)_{12}]$ with 1-ethynylcycloheptanol

Isolation by preparative TLC afforded the first fraction, which gave brown crystals of **3** after recrystallisation from a solution of pure *n*-hexane by slow evaporation at −10°C. The positive FAB mass spectrum exhibits a peak envelope at *m*/*z* 1146, which is followed by a series of peaks corresponding to the loss of carbonyl ligands. The IR spectrum reveals a band at 1856 cm^{-1} due to the presence of bridging carbonyl ligand. The ^{1}H-NMR spectrum of **3** recorded in $CDCl_3$ displays a series of multiplets in the range δ 0.70–3.02 integrating for 10 methylene protons. A quartet signal centred at δ 5.79 with *J*(HH) 6.2 Hz is assigned to the proton on C(24), which is coupled to two magnetically non-equivalent methylene protons on C(23). Furthermore, a downfield singlet resonance at δ 6.08 corresponds to the methine proton on C(17). An ORTEP diagram of the molecular structure of **3** is shown in Fig. 3. Table 3 gives some important bond parameters. The metal framework of **3** comprises a distorted octahedron in which the Ru–Ru bond lengths fall into the range 2.725(1)–3.081(1) Å with the Ru(1)–Ru(3) separation being the shortest and the Ru(1)–Ru(4) vector the longest. The Ru–C(carbide) bond distances range from 2.04(4) to 2.08(4) Å. Again, the carbide atom probably originates from the alkyne carbon atom, as one carbon is missing from the total in the reactant alkyne. An interstitial carbido atom occupies the central cavity and the organic molecule bridges the Ru(1)–Ru(4) edge of the cluster with one carbon atom bond to Ru(1) and three bonded to Ru(4), via σ and π-allyl interactions, respectively. The coordination sphere of the cluster is completed by 13 terminal CO ligands and one bridging CO ligand located on the same triangular face as the organic ligand, whereas in **1** the bridging CO ligand was on an edge of the opposite face. The alkyne moiety bonded to two Ru atoms adopts a μ_2-η^1,η^3 manner based upon the C≡C triple bond fissure. The carbon atom C(17) is bound to Ru(3) with a strong σ-bonding [Ru(3)–C(17) 2.09(4) Å], which together with C(18) and C(24) forms a η^3-allyl bonding mode to Ru(1) caused by both the C–H activation and hydroxyl elimination. An interesting feature of a flipped cycloheptyne ring is the chair conformation. The organic

Table 2
Some selected bond lengths (Å) and angles (°) for cluster **2**

Bond lengths (Å)			
Ru(1)–Ru(1)	2.868(1)	Ru(1)–Ru(2)	2.894(1)
Ru(1)–Ru(3)	3.077(1)	Ru(1)–Ru(3)	2.838(1)
Ru(2)–Ru(2)	2.869(1)	Ru(2)–Ru(3)	2.841(1)
Ru(1)–C(8)	2.19(4)	Ru(1)–C(11)	2.03(1)
Ru(2)–C(8)	2.23(1)	Ru(2)–C(8)	2.08(1)
Ru(3)–C(8)	2.16(4)	Ru(3)–C(9)	2.22(1)
Ru(3)–C(10)	2.25(1)	Ru(3)–C(11)	2.26(1)
C(8)–C(9)	1.43(1)	C(9)–C(10)	1.40(1)
C(10)–C(11)	1.42(1)	C(10)–C(14)	1.52(1)
C(11)–C(12)	1.51(1)	C(12)–C(13)	1.53(1)
C(13)–C(14)	1.50(1)		
Bond angles (°)			
Ru(3)–Ru(1)–Ru(3)	115.7(2)	Ru(1)–Ru(2)–Ru(3)	64.9(1)
C(8)–Ru(1)–C(11)	75.9(2)	C(8)–Ru(3)–C(9)	38.2(2)
C(9)–Ru(3)–C(10)	36.5(2)	C(10)–Ru(3)–C(11)	36.8(2)

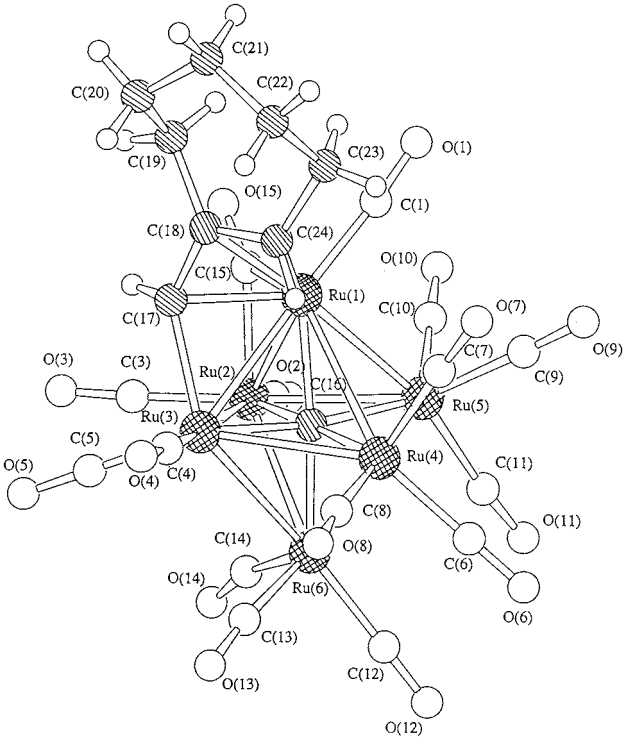

Fig. 3. Molecular structure of cluster **3**.

fragment is counted as a six-electron donor so as to achieve 86 CVEs for cluster **3**.

The molecular structure of compound **4** is depicted in Fig. 4 along with the atomic numbering scheme. The selected interatomic distances and angles are shown in Table 4. In contrast to the typical six metal atoms with eight M–M bonds [27], the metal skeleton of **4** comprises two distorted square planar units with one additional edge bridging Ru(2) and Ru(3). The Ru–Ru bond lengths lie in the range 2.829(1)–2.899(1) Å. Again, the structure of **4** is symmetric and possesses a crystallographic two-fold rotation axis passing through Ru(2) and Ru(2*). The bonding mode of the two alkyne ligands is similar to that in cluster **2**. It is interesting that the two flipped cycloheptyne rings adopt a chair conformation. If each organic fragment is considered to be an eight-electron donor, cluster **4** has 92 CVEs, which obeys the EAN rule for six ruthenium atoms having eight metal–metal bonds. The spectroscopic data for **4** are fully consistent with the solid-state structure (see Table 8). The positive FAB mass spectrum shows a peak envelope at m/z 1237, consistent with an isotopic distribution of six Ru atoms. The ^{1}H-NMR spectrum of **4** in $CDCl_3$ exhibits several multiplets in the range δ 1.78–2.82 due to the 20 methylene protons on the two C_7 rings and a considerable downfield singlet at δ 5.32 assigned to two methine proton on C(9) and C(9*), respectively. Furthermore, the IR spectrum reveals the presence of terminal carbonyl ligands only.

Table 3
Some selected bond lengths (Å) and angles (°) for cluster **3**

Bond lengths (Å)			
Ru(1)–Ru(2)	2.825(1)	Ru(1)–Ru(3)	2.725(1)
Ru(1)–Ru(4)	3.081(1)	Ru(1)–Ru(5)	2.843(1)
Ru(2)–Ru(3)	2.942(1)	Ru(2)–Ru(5)	2.882(1)
Ru(3)–Ru(4)	2.973(1)	Ru(4)–Ru(5)	2.848(1)
Ru(2)–Ru(6)	2.862(1)	Ru(3)–Ru(6)	2.979(1)
Ru(4)–Ru(6)	2.836(1)	Ru(5)–Ru(6)	3.003(1)
Ru(1)–C(15)	2.12(1)	Ru(1)–C(16)	2.04(4)
Ru(1)–C(17)	2.16(4)	Ru(1)–C(18)	2.24(4)
Ru(1)–C(24)	2.27(4)	Ru(2)–C(15)	2.06(5)
Ru(2)–C(16)	2.08(4)	Ru(3)–C(16)	2.04(4)
Ru(3)–C(17)	2.09(4)	Ru(4)–C(16)	2.05(4)
Ru(5)–C(16)	2.05(4)	C(17)–C(18)	1.41(1)
C(18)–C(19)	1.52(1)	C(18)–C(24)	1.41(1)
C(19)–C(20)	1.53(1)	C(20)–C(21)	1.52(1)
C(21)–C(22)	1.53(2)	C(22)–C(23)	1.54(1)
C(23)–C(24)	1.51(1)		
Bond angles (°)			
Ru(1)–C(17)–Ru(3)	79.7(2)		
C(17)–Ru(1)–C(18)	37.3(2)	C(18)–Ru(1)–C(24)	36.5(2)

2.3. Treatment of $[Ru_3(CO)_{12}]$ with 1-ethynylcycloctanol

The molecular structure of **5** was established by X-ray crystallography and is shown in Fig. 5. Table 5 collects some important bond parameters. The spectroscopic data for **5** are fully consistent with the solid-state structure (see Table 8). An intense molecular ion peak at m/z 1285 was observed in the positive FAB mass spectrum. The IR spectrum shows CO stretches between 2074 and 1876 cm^{-1}, which are typical of terminal and bridging carbonyl groups. The ^{1}H-NMR spectrum of **5** contains a number of multiplets, which are integrated to give a total of 26 proton resonances. Three methine protons give rise to three resonances centred at δ 4.52, 4.06 and 1.14. The signal at δ 4.52 is a doublet with J(HH) 7.6 Hz and corresponds to the proton on C(26). The resonance at δ 4.06 is a triplet with J(HH) 7.6 Hz and corresponds to the proton on C(25). The signal at δ 1.14 is also a doublet with J(HH) 7.6 Hz and may be assigned to the other methine proton on C(24). A more persuasive assignment was obtained by performing the DEPT ^{13}C- and normal ^{13}C-NMR experiments. The DEPT ^{13}C-NMR spectrum of **5** clearly shows the 13 methylene and three methine carbon resonances in the δ 21.30–54.04 region. The well-resolved ^{13}C-NMR spectrum of **5** provides evidence for one alkoxy and two acetylenic carbon atom resonances, and five resonances are also observed in the δ 197.85–216.63 region indicative of carbonyl scrambling over the metal cluster (see Table 8). The compound has also been analysed using a

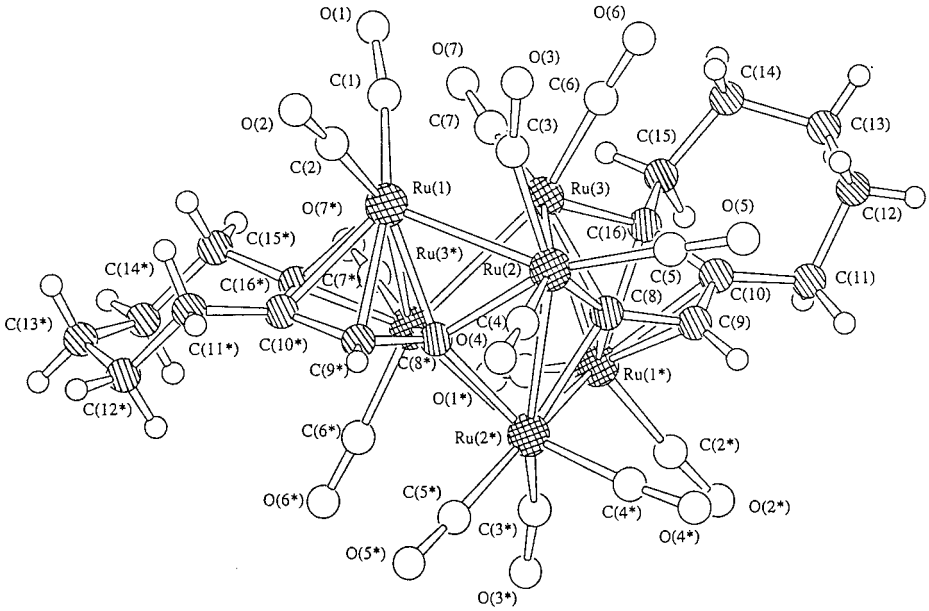

Fig. 4. Molecular structure of cluster **4**.

combination of 2D ^{1}H-^{1}H-COSY, 2D ^{13}C-^{1}H-COSY, 2D NOESY (nuclear Overhauser enhancement spectroscopy) and COLOC (C–H correlation spectroscopy via long-range couplings) experiments, which suggests that the pairs of signals arise from the geminal protons of each cyclooctyne ring system. Figs. 8 and 9 present the basic ^{1}H-NMR spectrum along with cross sections as indicated on the plot of the COSY and NOESY experiments. Furthermore, signal assignment has also been confirmed from a TOCSY (total correlation spectroscopy) experiment [28,29] as shown in Fig. 10. The probable assignments of the protons and the carbon atoms for **5** are summarised in Table 10. The Ru–Ru bond distances range from 2.763(1) to 3.009(1) Å and the Ru–C(carbide) bond distances are 2.02(1)–2.10(1) Å in **5**. The ligand capped on the Ru(1)–Ru(2)–Ru(3) triangular face is different from those observed in other related carbido–hexruthenium clusters such as $Ru_6C(CO)_{15}$(MeCH=CH–CH=CHMe)] [30] with 2,4-hexadiene molecule and [Ru_6C-$(CO)_{14}(CH_2CHCH\text{-}CHCHCH_2)$] [31] with 1,3,5-hexatriene ligand. Dimerization of the starting functionalized alkyne units generates a substituted 1,2,-3,4-hexatetraene chain followed by water elimination. In **5**, the resulting ligand bonded to the Ru(1)–Ru(4)–Ru(5) triangular face is similar to those observed in cluster **1** with a combination of a η^3-allyl, σ- and π-interaction. The average Ru–Ru bond distance of the Ru_3 face [Ru(1)–Ru(4)–Ru(5)] in **5** [2.894(1) Å] is slightly longer than in **1** [average 2.807(3) Å], which may reflect the difference number of carbon atoms coordinated to the Ru_3 face. The bond lengths of the ligand-bridged Ru–Ru edges [average 2.807(3) Å for **1**; 2.894(1) Å for **5**] are found to be significantly shorter than any of the other Ru–Ru bonds [average 2.929(4) Å for **1**; 2.909(7) Å for **5**], which has also been observed in the related hexa-ruthenium carbido clusters [31,32]. The ring carbon atom C(16) undergoes C–H activation to form a σ bond to Ru(4) [Ru(4)–C(16) 2.10(1) Å], which also forms a π interaction to Ru(5) with its adjacent ring carbon atom C(23) [C(16)–C(23) 1.42(1) Å] followed by the loss of a hydroxy group. This cyclooctyne ring, C(16)–C(17)–C(18)–C(19)–C(20)–C(21)–C(22)–C(23), espouses a chair conformation which is closely related to that of [$Ru_6C(CO)_{15}(\mu_3$-η^1,η^1,η^2-$C_8H_{12})$] [33]. The alkyne carbon atom C(24) is coupled to another alkyne moiety, C(25) and C(26),

Table 4
Some selected bond lengths (Å) and angles (°) for cluster **4**

Bond lengths (Å)			
Ru(1)–Ru(2)	2.829(1)	Ru(1)–Ru(3)	2.850(1)
Ru(2)–Ru(2)	2.860(1)	Ru(2)–Ru(3)	2.899(1)
Ru(3)–Ru(3)	2.840(1)	Ru(1)–C(8)	2.14(3)
Ru(1)–C(9)	2.20(4)	Ru(1)–C(10)	2.26(4)
Ru(1)–C(16)	2.22(4)	Ru(2)–C(8)	2.10(4)
Ru(2)–C(8)	2.22(4)	Ru(3)–C(8)	2.16(4)
Ru(3)–C(16)	2.06(4)	C(8)–C(9)	1.42(5)
C(9)–C(10)	1.42(6)	C(10)–C(11)	1.52(6)
C(10)–C(16)	1.42(6)	C(11)–C(12)	1.53(1)
C(12)–C(13)	1.50(1)	C(13)–C(14)	1.51(1)
C(14)–C(15)	1.53(1)	C(15)–C(16)	1.51(1)
Bond angles (°)			
Ru(1)–Ru(2)–Ru(3)	64.7(1)	Ru(2)–Ru(1)–Ru(3)	83.3(1)
Ru(2)–Ru(2)–Ru(3)	81.9(10)	C(8)–Ru(3)–C(16)	76.8(2)
C(8)–Ru(1)–C(9)	38.0(1)	C(9)–Ru(1)–C(10)	37.1(1)
C(10)–Ru(1)–C(16)	37.0(1)		

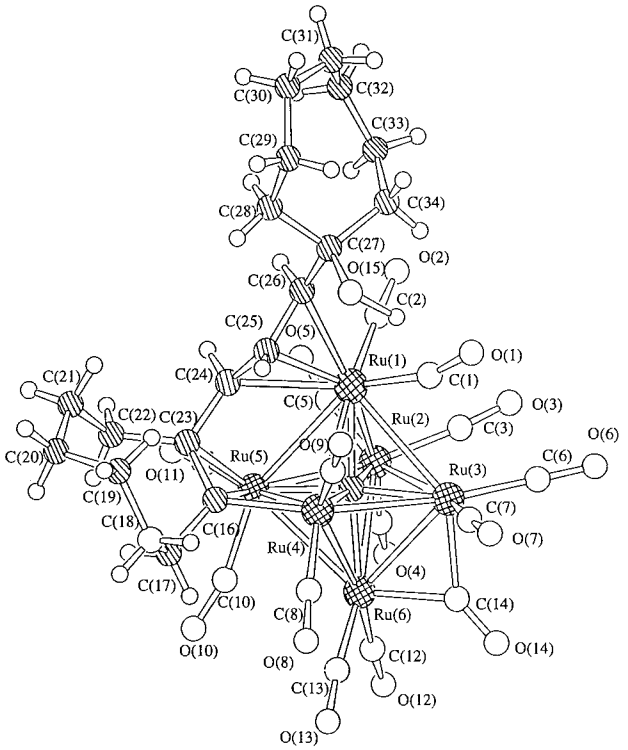

Fig. 5. Molecular structure of cluster **5**.

to afford a η^3-allyl ligand [C(24)–C(25) 1.43(1) Å, C(25)–C(26) 1.40(1) Å] bound to Ru(1), via a combination of C≡C triple bond cleavage, C≡C triple bond and C–H bond activations. Like **1** and **3**, a μ_6-carbide is also believed to originate from the alkyne carbon. Regarding the resulting ligand as a six electron donor, the valence-electron count is 86 for **5**, which is in agreement with the PSEPT rule.

Characterization of compound **6** has been achieved from spectroscopic evidence and its structure confirmed by single-crystal X-ray diffraction analysis (Table 6). The molecular structure of **6** is shown in Fig. 6. As far as the metal core geometry and the distribution of CO ligand and the alkynyl moieties are concerned, they are essential identical to **4**. The IR spectrum exhibits CO stretches between 2072 and 1948 cm^{-1}, which are typical of terminal carbonyl groups (see Table 8). The mass spectrum gives a strong parent peak at m/z 1265. Its ^{1}H-NMR spectrum recorded in $CDCl_3$ comprises a series of multiplets in the δ 1.74–2.87 region corresponding to the 24 methylene protons on the two cyclooctyne rings, as well as a singlet signal at δ 5.33 attributable to the two methine protons on C(9 and 9*). Both the metal framework and bonding mode of the alkyne ligands are essentially the same as those in cluster **4**. The two metallated five-membered rings are approximately planar with a maximum deviation of 0.18 Å, which are similar to that observed in **4** [0.21 Å]. Again, the two C_8H_{12} rings are arranged in a chair conformation. The valence-electron count is 92 for **6**, which is in agreement with the EAN rule.

Table 5
Some selected bond lengths (Å) and angles (°) for cluster **5**

Bond lengths (Å)			
Ru(1)–Ru(2)	2.819(1)	Ru(1)–Ru(3)	2.962(1)
Ru(1)–Ru(4)	2.909(1)	Ru(1)–Ru(5)	3.009(1)
Ru(2)–Ru(3)	2.971(1)	Ru(2)–Ru(5)	2.866(1)
Ru(2)–Ru(6)	2.936(2)	Ru(3)–Ru(4)	2.946(1)
Ru(3)–Ru(6)	2.777(1)	Ru(4)–Ru(5)	2.763(1)
Ru(4)–Ru(6)	2.979(1)	Ru(5)–Ru(6)	2.927(1)
Ru(1)–C(15)	2.06(1)	Ru(1)–C(24)	2.50(1)
Ru(1)–C(25)	2.22(1)	Ru(1)–C(26)	2.33(1)
Ru(2)–C(15)	2.04(1)	Ru(3)–C(14)	2.03(1)
Ru(3)–C(15)	2.02(1)	Ru(4)–C(15)	2.02(1)
Ru(4)–C(16)	2.10(1)	Ru(5)–C(15)	2.06(1)
Ru(5)–C(16)	2.24(2)	Ru(5)–C(23)	2.18(2)
Ru(6)–C(14)	2.06(1)	Ru(6)–C(15)	2.10(1)
C(16)–C(17)	1.49(2)	C(16)–C(23)	1.42(1)
C(17)–C(18)	1.52(2)	C(18)–C(19)	1.53(2)
C(19)–C(20)	1.55(2)	C(20)–C(21)	1.53(2)
C(21)–C(22)	1.52(2)	C(22)–C(23)	1.54(1)
C(23)–C(24)	1.45(1)	C(24)–C(25)	1.43(1)
C(25)–C(26)	1.40(1)	C(26)–C(27)	1.53(1)
C(27)–C(28)	1.54(2)	C(27)–C(34)	1.55(2)
C(28)–C(29)	1.54(2)	C(29)–C(30)	1.49(2)
C(30)–C(31)	1.47(3)	C(31)–C(32)	1.42(3)
C(32)–C(33)	1.48(3)	C(33)–C(34)	1.45(2)
C(27)–O(15)	1.40(1)		
Bond angles (°)			
C(24)–Ru(1)–C(25)	34.8(3)		
C(25)–Ru(1)–C(26)	35.8(4)	C(16)–Ru(2)–C(23)	37.5(4)
C(23)–C(24)–C(25)	121(1)	C(24)–C(25)–C(26)	121(1)
C(25)–C(26)–C(27)	121(1)		

Table 6
Some selected bond lengths (Å) and angles (°) for cluster **6**

Bond lengths (Å)			
Ru(1)–Ru(2)	2.836(1)	Ru(1)–Ru(3)	2.891(1)
Ru(2)–Ru(2)	2.843(1)	Ru(2)–Ru(3)	2.862(1)
Ru(3)–Ru(3)	2.862(1)	Ru(1)–C(8)	2.24(1)
Ru(1)–C(9)	2.09(1)	Ru(1)–C(10)	2.16(1)
Ru(1)–C(11)	2.20(1)	Ru(2)–C(8)	2.25(1)
Ru(2)–C(8)	2.24(1)	Ru(3)–C(8)	2.14(1)
Ru(3)–C(11)	2.07(1)	C(8)–C(9)	1.42(1)
C(9)–C(10)	1.42(1)	C(10)–C(11)	1.54(1)
C(10)–C(17)	1.43(1)	C(11)–C(12)	1.52(1)
C(12)–C(13)	1.53(1)	C(13)–C(14)	1.52(1)
C(14)–C(15)	1.54(1)	C(15)–C(16)	1.53(9)
C(16)–C(17)	1.48(9)		
Bond angles (°)			
Ru(1)–Ru(2)–Ru(3)	65.4(2)		
Ru(2)–Ru(1)–Ru(3)	83.3(2)	C(8)–Ru(1)–C(9)	38.1(2)
C(9)–Ru(1)–C(10)	37.3(2)	C(10)–Ru(1)–C(11)	37.1(2)

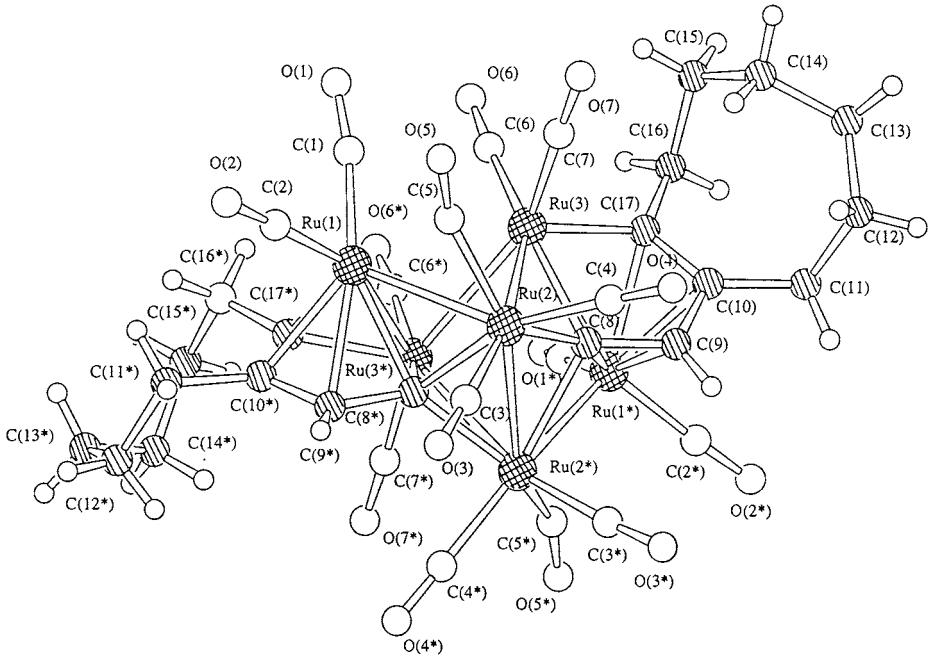

Fig. 6. Molecular structure of cluster **6**.

2.4. Reaction of $[Ru_3(CO)_{10}(NCMe)_2]$ with 1-ethynylcyclpentanol

A dichloromethane solution of $[Ru_3(CO)_{10}(NCMe)_2]$ was stirred at room temperature with one molar equivalent of 1-ethynylcyclopentanol. This resulted in a darkening of the solution and subsequent work up results in the isolation of a single product $[Ru_3(CO)_9(\mu\text{-}CO)(\mu_3\text{-}\eta^1,\eta^1,\eta^2\text{-}HCC\{C_5H_8OH\})]$ **7** (20% yield). A single crystal grown from an *n*-hexane solution of **7** was subjected to an X-ray crystallographic analysis. The molecular structure of **7** in the solid state is illustrated in Fig. 7 together with the atomic labelling scheme. Some important bond parameters are given in Table 7. The molecular structure of **7** consists of a closed triruthenium unit, with Ru–Ru bond lengths ranging from 2.703(1) to 2.835(1) Å, capped by a 1-ethynylcy clopentanol ligand in a classical μ_3-η^2 manner. This creates the nido-octahedral M_3C_2 core geometry expected for this type of coordination. The Ru_3 triangular unit is coordinated by nine terminally bound and a single asymmetrically bridging carbonyl ligands, the latter bridging the Ru(2)–Ru(3) edge. The Ru-bound alkyne bond length, C(11)–C(12), shows a characteristic lengthening to 1.39(1) Å, as expected for a μ_3-η^2 bound alkyne unit. It should be noted that the cyclopentyl ring is skewed to avoid the undesirable conflict between the protons located on C(11) and C(14). In conclusion, the coordination mode observed in **7** is similar to those observed in the reaction products of dialkyl and diaryl acetylenes with activated derivatives of $[Ru_3(CO)_{12}]$ [34,35]. The spectroscopic data for compound **7** are fully consistent with its solid-state structure. The mass spectrum shows a parent peak at m/z 694 followed by the sequential loss of 10 CO groups (Table 8). The ^{1}H-NMR spectrum recorded in $CDCl_3$ displays two sets of multiplets in the range δ 1.55–2.03 for the eight methylene protons and a downfield singlet

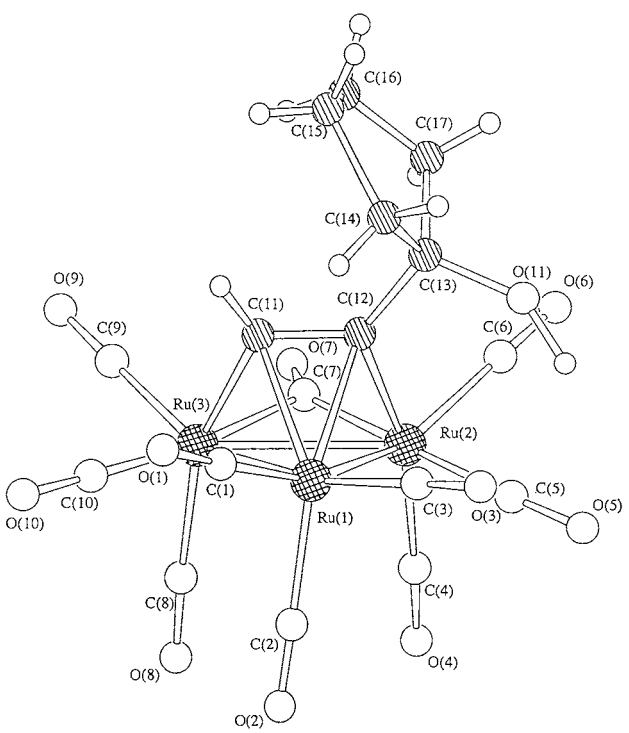

Fig. 7. Molecular structure of cluster **7**.

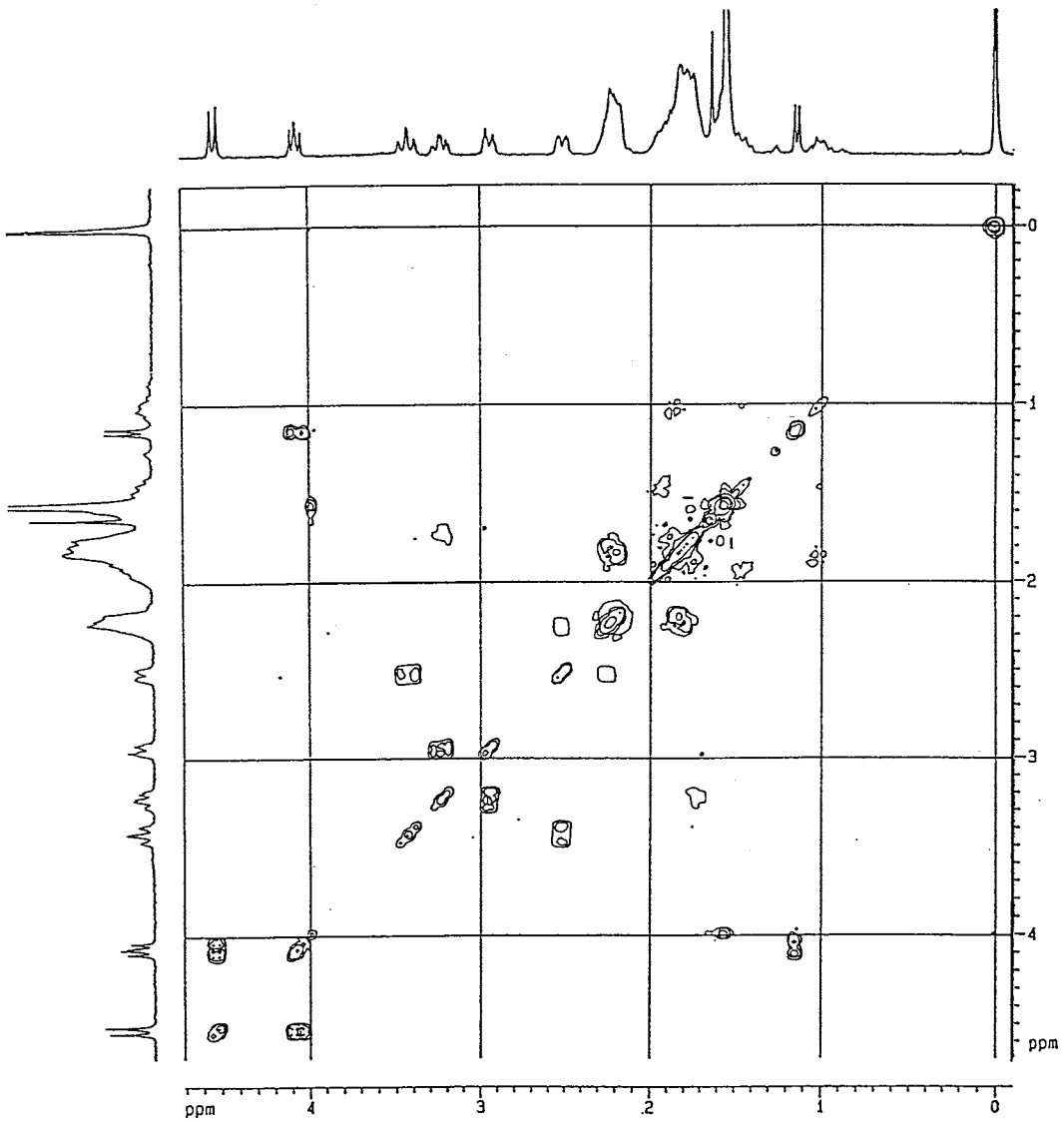

Fig. 8. 2D COSY spectrum of **5** with the ^{1}H-NMR plot along the cross section in 300 MHz.

signal at δ 8.22 due to the acetylenic proton. However, no hydroxyl signal is observed. The IR spectrum reveals six absorptions in the range 2068–1850 cm^{-1}.

3. Experimental

All the reactions were performed in an atmosphere of high-purity nitrogen using standard Schlenk techniques. Analytical grade solvents were purified by distillation over the appropriate drying agents and in an inert nitrogen atmosphere prior to use. Infrared spectra were recorded on a Bio-Rad FTS-7 spectrometer using a 0.5 mm solution cell. Positive-ion fast atom bombardment mass spectra were obtained using a Finnigan MAT 95 spectrometer. ^{1}H-NMR and ^{13}C-NMR spectra were recorded in $CDCl_3$ on a Bruker DPX 300 and DRX 500 NMR instrument, referenced to internal $SiMe_4$ ($\delta = 0$). The reactions were monitored by analytical thin-layer chromatography (5735 Kieselgel 60 F_{254}, E. Merck) and the products were separated on preparative thin-layer chromatographic plates coated with Merck Kieselgel 60 GF_{254}. The starting compounds 1-ethynylcyclopentanol, 1-ethynylcycloheptanol and 1-ethynylcyclooctanol were obtained from Lancaster and used without further purification.

4. Synthesis

4.1. Reaction of $[Ru_3(CO)_{12}]$ with 1-ethynylcyclopentanol in refluxing cyclohexane

The compound $[Ru_3(CO)_{12}]$ (0.100 g, 0.15 mmol) was refluxed with 1-ethynylcyclopentanol (0.017 g, 0.15

mmol) in cyclohexane (60 ml) for 12 h. The solvent was removed in vacuo and the residue separated by TLC using dichloromethane–hexane (15:85 v/v) as eluent to afford two bands with R_f values of 0.45 and 0.80. Clusters **1** (R_f 0.45) and **2** (R_f 0.80) were isolated as solids in 12 and 8% yields, respectively. (Found for **1** $Ru_6C_{28}H_{16}O_{14}$: C, 28.61; H, 1.56. Anal. Calc.: C, 28.43; H, 1.37%. Found for **2** $Ru_6C_{28}H_{14}O_{14}$: C, 28.59; H, 1.30. Anal. Calc.: C, 28.47; H, 1.19%).

4.2. Reaction of $[Ru_3(CO)_{12}]$ with 1-ethynylcycloheptanol in refluxing cyclohexane

The compound $[Ru_3(CO)_{12}]$ (0.100 g, 0.15 mmol) was refluxed with 1-ethynylcycloheptanol (0.022 g, 0.15 mmol) in cyclohexane (60 ml) for 12 h. The solvent was removed in vacuo and the residue separated by TLC using dichloromethane–hexane (15:85 v/v) as eluent to afford two bands with R_f values of 0.50 and 0.85. Clusters **3** (R_f 0.50) and **4** (R_f 0.85) were isolated as solids in 8 and 10% yields, respectively. (Found for **3** $Ru_6C_{24}H_{12}O_{15}$: C, 25.35; H, 1.25. Anal. Calc.: C, 25.15; H, 1.06%. Found for **4** $Ru_6C_{32}H_{22}O_{14}$: C, 31.15; H, 1.98. Anal. Calc.: C, 31.07; H, 1.79%).

4.3. Reaction of $[Ru_3(CO)_{12}]$ with 1-ethynylcyclooctanol in refluxing cyclohexane

The compound $[Ru_3(CO)_{12}]$ (0.100 g, 0.15 mmol) was refluxed with 1-ethynylcyclooctanol (0.024 g, 0.15 mmol) in cyclohexane (60 ml) for 12 h. The solvent was removed in vacuo and the residue separated by TLC using dichloromethane–hexane (15:85 v/v) as eluent to afford two bands with R_f values of 0.40 and 0.75.

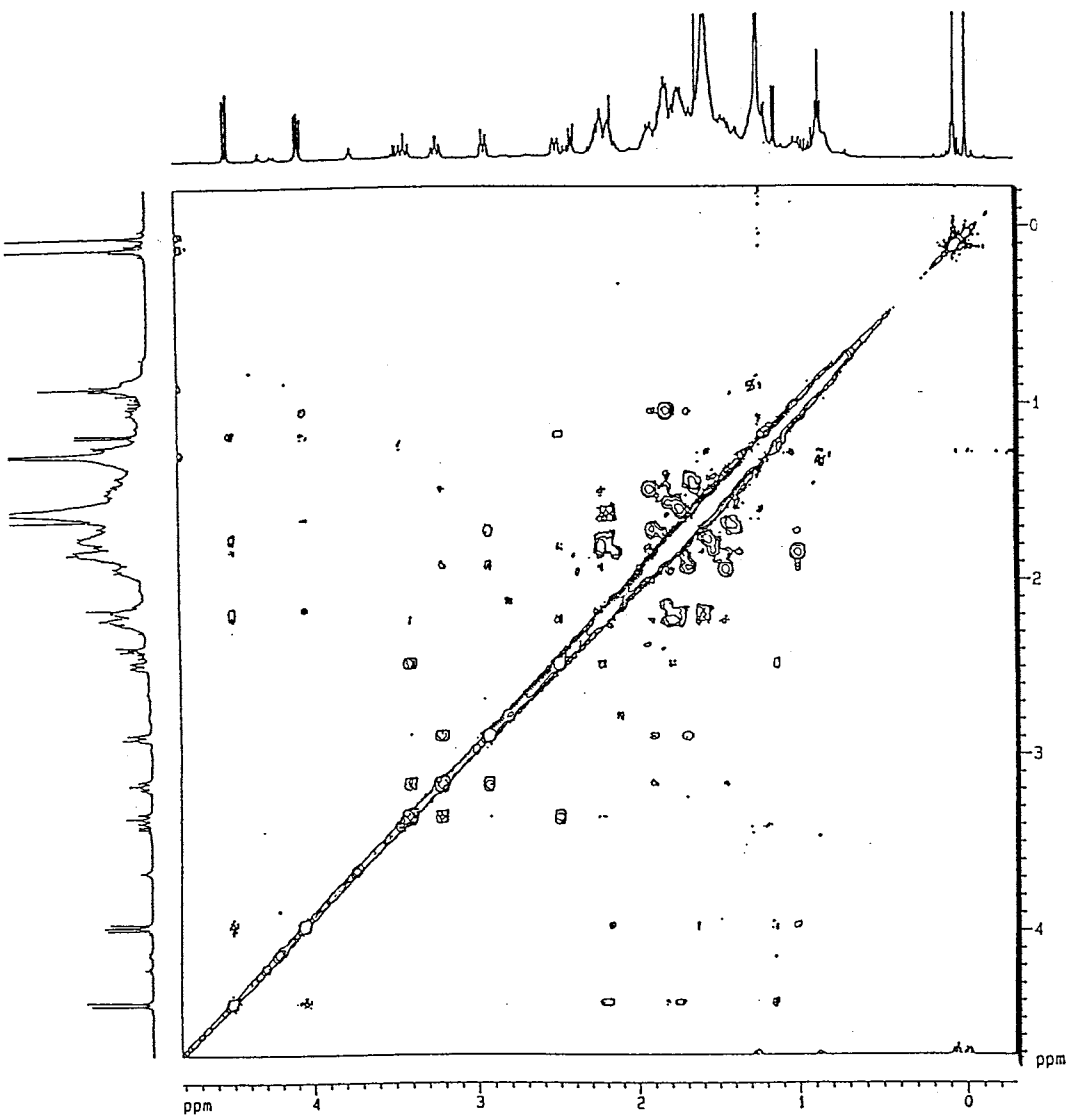

Fig. 9. 2D NOESY spectrum of **5** with the ^{1}H-NMR plot along the cross section in 500 MHz.

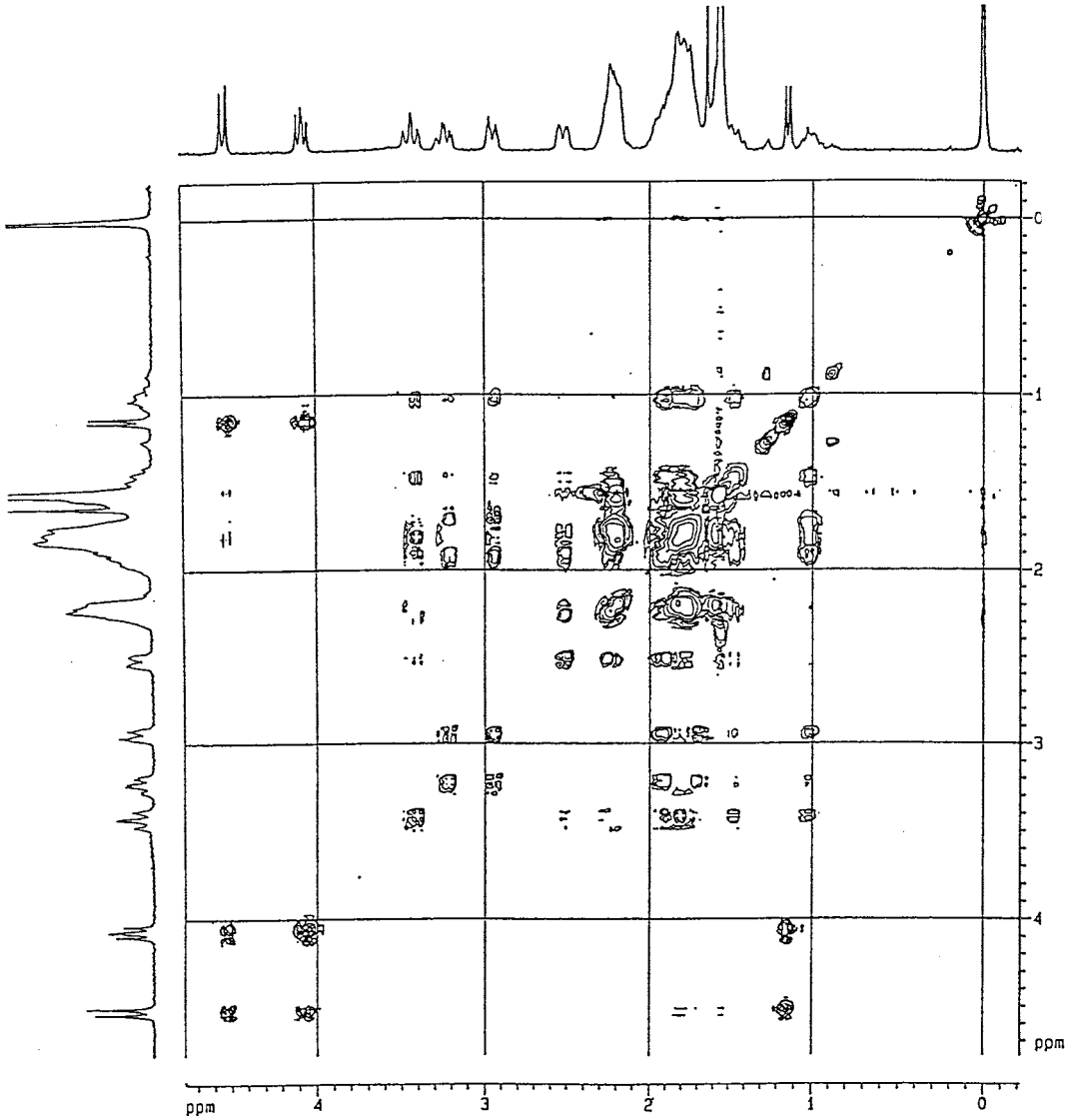

Fig. 10. 2D TOCSY spectrum of **5** with the ^{1}H-NMR plot along the cross section in 300 MHz.

Clusters **5** (R_f 0.40) and **6** (R_f 0.75) were isolated as solids in 16 and 8% yields, respectively. (Found for **5** $Ru_6C_{35}H_{30}O_{15}$: C, 31.95; H, 2.50 Anal. Calc.: C, 31.78; H, 2.36%. Found for **6** $Ru_6C_{34}H_{26}O_{14}$: C, 32.42; H, 2.31. Anal. Calc.: C, 32.28; H, 2.07%).

4.4. Reaction of $[Ru_3(CO)_{10}(NCMe)_2]$ with 1-ethynylcyclopentanol

The compound $[Ru_3(CO)_{10}(NCMe)_2]$ [36] (0.085 g, 0.13 mmol) was stirred with 1-ethynylcyclopentanol (0.014 g, 0.13 mmol) in dichloromethane (60 ml) for 1 h at room temperature. Infrared spectroscopy and TLC indicated complete consumption of the starting material. The solvent was removed in vacuo and the residue separated by TLC using dichloromethane–hexane (20:80 v/v) as eluent to afford one band with R_f value of 0.50. The cluster **7** was isolated as an orange

Table 7
Some selected bond lengths (Å) and angles (°) for cluster **7**

Bond lengths (Å)			
Ru(1)–Ru(2)	2.745(1)	Ru(1)–Ru(3)	2.703(1)
Ru(2)–Ru(3)	2.835(1)	Ru(1)–C(11)	2.23(8)
Ru(1)–C(12)	2.25(1)	Ru(2)–C(7)	2.06(2)
Ru(2)–C(12)	2.12(1)	Ru(3)–C(7)	2.28(2)
Ru(3)–C(11)	2.07(1)	C(11)–C(12)	1.39(1)
C(12)–C(13)	1.51(1)	C(13)–C(14)	1.53(1)
C(13)–C(17)	1.54(1)	C(14)–C(15)	1.65(3)
C(15)–C(16)	1.42(3)	C(16)–C(17)	1.46(2)
Bond angles (°)			
Ru(1)–Ru(2)–Ru(3)	57.9(2)	Ru(2)–Ru(1)–Ru(3)	62.7(3)
Ru(1)–Ru(3)–Ru(2)	59.3(2)	Ru(1)–C(12)–Ru(2)	77.7(3)
Ru(1)–C(11)–Ru(3)	77.8(3)	Ru(1)–C(11)–C(12)	72.7(5)
Ru(1)–C(12)–C(11)	71.2(5)		

Table 8
Spectroscopic data for clusters **1**–**7**

Cluster	IR, ν(CO) (cm^{-1}) [a]	NMR, δ J (Hz) [b]	MS m/z [c]
1	2074w, 2051vs, 2037s, 2027s, 2010w, 1993w, 1845m	^{1}H: 5.61 (1H, q, $J = 5.8$ Hz), 3.66 (1H, s), 3.58–3.38 (3H, m), 2.75–2.55 (5H, m), 2.18–1.86 (6H, m)	1183(1183)
2	2072m, 2039w, 1966w, 2020vs, 2006s, 1993s, 1835w	^{1}H: 5.30 (2H, s), 2.85–2.78 (2H, m), 2.75–2.30 (4H, m), 2.28–2.16 (2H, m), 2.14–2.10 (2H, m), 1.97–1.84 (2H, m)	1181(1181)
3	2085w, 2049s, 2037s, 2025w, 2008m, 1992w, 1856w	^{1}H: 6.08 (1H, s), 5.79 (1H, q, $J = 6.2$ Hz), 3.02–2.94 (1H, m), 2.76–2.69 (1H, m), 2.49–2.43 (1H, m), 1.99–1.94 (1H, m), 1.73–1.62 (2H, m), 1.48-1.46 (1H, m), 1.35–1.30 (1H, m), 0.90–0.86 (1H, m), 0.78–0.70 (1H, m)	1146(1146)
4	2073w, 2037s, 2021vs, 2002s, 1991m	^{1}H: 5.32 (2H, s), 2.82–2.77 (2H, m), 2.75–2.70(2H, m), 2.55–2.46 (4H, m), 2.36–2.27 (2H, m), 2.18–2.10 (3H, m), 2.00–1.93 (3H, m), 1.90–1.78 (4H, m)	1237(1237)
5	2074m, 2051vs, 2033s, 2027s, 2002s, 1876w	^{1}H: 4.54–4.51 (1H, d, $J = 7.6$ Hz), 4.09–4.04 (1H, t, $J = 7.6$ Hz), 3.47–3.38 (1H, m), 3.27–3.18 (1H, m), 2.96–2.92 (1H, m), 2.53–2.49 (1H, m), 2.30–2.10 (5H, m), 1.95–1.80 (1H, m), 1.79–1.62 (14H, m), 1.38–1.30 (1H, m), 1.15–1.13 (1H, d, $J = 7.6$ Hz), 1.03–0.99 (1H, m) ^{13}C: 216.63, 202.73, 200.66, 198.42, 197.85, 99.05, 92.65, 76.24, 54.04, 48.09, 42.06, 41.93, 37.74, 33.75, 32.99, 29.84, 28.29, 27.89, 27.25, 25.18, 25.01, 23.17, 22.33, 21.30	1285(1285)
6	2072w, 2035s, 2025s, 2000m, 1948w	^{1}H: 5.33 (2H, s), 2.87–2.80 (2H, m), 2.74–2.68(2H, m), 2.61–2.54 (2H, m), 2.32–2.20 (4H, m), 2.19–2.09 (4H, m), 2.01–1.88 (5H, m), 1.86–1.74 (5H, m)	1265(1265)
7	2068s, 2040s, 2005vs, 1950s, 1850w	^{1}H: 8.22 (1H, s), 2.03–1.81 (4H, m), 1.78–1.55 (4H, m)	694(694)

[a] CH_2Cl_2.
[b] $CDCl_3$.
[c] Simulated values given in parentheses.

solid in 20% yield. (Found for **3** $Ru_3C_{17}H_{10}O_{11}$: C,29.54; H, 1.56. Anal. Calc.: C, 29.42; H, 1.45%).

*4.5. X-ray data collection and structural determination of complexes **1**–**7***

Crystals of all new complexes suitable for X-ray analyses were mounted on top of a glass fibre using epoxy resin or Lindermann glass capillary (**1** and **2**). Intensity data were collected at ambient temperature either on a MAR Research image plate scanner (for **1**–**6**) or a Rigaku AFC7R diffractometer (for **7**) with graphite-monochromated Mo–K_α radiation ($\lambda =$ 0.71073 Å) using ω scan and $\omega - 2\theta$ scan techniques, respectively. A summary of the crystallographic data and structure refinement is listed in Table 9. All intensity data were collected for Lorentz and polarization effects. The Ψ-scan method was employed for semi-empirical absorption corrections for **7** however, an approximation to absorption correction by inter-image scaling was applied for **1**–**6**. Scattering factors were taken from Ref. [37a] and anomalous dispersion effects [37b] were included in F_c. The structures were solved by a combination of direct methods (SHELXS-86 [38] for **1**, **3** and **4**; SIR 88 [39] for **2** and **5**–**7**) and Fourier difference techniques and refined on F by full-matrix least-squares analysis. The hydrogen atoms of the organic moieties were generated in their ideal positions (C–H 0.95 Å). All calculations were performed on a Silicon-Graphics computer, using the program package TEXSAN [40]. Additional material available from the Cambridge Crystallographic Data Centre (CCDC) comprises final atomic coordinates, thermal parameters and all bond parameters. CCDC deposition numbers are 119742 to 119748.

Acknowledgements

We gratefully acknowledge the financial support for this work by the Hong Kong Research Grants Council and the University of Hong Kong; C.S.-W.L. also acknowledges the receipt of a postgraduate studentship administered by the University of Hong Kong.

Table 9
Summary of crystal data and data collection parameters for clusters **1**–**7**

Cluster	**1**	**2**	**3**	**4**	**5**	**6**	**7**
Empirical formula	$Ru_6C_{28}H_{16}O_{14}\cdot\frac{1}{2}C_2H_6O$	$Ru_6C_{28}H_{14}O_{14}\cdot CH_2Cl_2$	$Ru_6C_{24}H_{12}O_{15}$	$Ru_6C_{32}H_{22}O_{14}$	$Ru_6C_{34}H_{30}O_{15}$	$Ru_6C_{34}H_{26}O_{14}$	$Ru_3C_{17}H_{10}O_{11}$
Molecular weight	1205.88	1265.76	1146.77	1236.94	1285.02	1264.99	693.47
Crystal colour, habit	Red, rod	Brown, rod	Red, rod	Red, plate	Brown, block	Red, plate	Orange, block
Crystal size (mm)	$0.14\times0.17\times0.31$	$0.13\times0.25\times0.29$	$0.25\times0.34\times0.37$	$0.16\times0.30\times0.31$	$0.25\times0.25\times0.26$	$0.15\times0.17\times0.32$	$0.29\times0.32\times0.36$
Crystal system	Triclinic	Monoclinic	Monoclinic	Monoclinic	Monoclinic	Monoclinic	Triclinic
Space group	$P\bar{1}$ (no. 2)	$C2/c$ (no. 15)	$P2_1/a$ (no. 14)	$C2/c$ (no. 15)	$P2_1/n$ (no. 14)	$C2/c$ (no. 15)	$P\bar{1}$ (no. 2)
a (Å)	11.244(1)	20.437(1)	17.557(1)	17.244(1)	13.049(1)	17.234(1)	9.891(3)
b (Å)	16.422(1)	10.158(1)	9.698(1)	9.642(2)	20.213(2)	9.687(1)	12.594(5)
c (Å)	20.881(1)	18.977(1)	18.601(1)	21.381(1)	15.019(1)	22.341(1)	8.829(4)
α (°)	111.31(2)	90	90	90	90	90	93.71(3)
β (°)	91.95(2)	100.61(2)	104.55(2)	97.69(2)	92.31(2)	94.53(2)	98.99(3)
γ (°)	99.04(2)	90	90	90	90	90	80.69(3)
V (Å^3)	3530.0(8)	3872.3(5)	3065.6(5)	3523.0(5)	3958.19(1)	3718.1(4)	1071.0(7)
Z	4	4	4	4	4	4	2
$D_{calc.}$ (g cm^{-3})	2.269	2.171	2.485	2.332	2.156	2.260	2.150
$F(000)$	2292	2400	2160	2360	2472	2424	664
μ(Mo–K_α) (cm^{-1})	25.68	24.79	29.51	25.76	22.99	24.43	21.44
2θ range collected (°)	2.0–51.2	2.0–51.2	2.0–51.2	2.0–51.2	2.0–51.2	2.0–51.2	2.0–51.2
No. of reflections collected	31329	10627	27126	10445	35219	11524	3003
No. of unique reflections	10822	3599	5815	3269	7556	3571	2806
No. of observed reflections [$I>3\sigma(I)$]	6948	3000	4359	2870	4951	2593	2367
R	0.075	0.034	0.025	0.028	0.065	0.036	0.043
R_w	0.081	0.040	0.032	0.036	0.074	0.043	0.054
Goodness-of-fit (S)	1.73	1.76	1.23	1.61	1.69	1.30	1.78
Maximum Δ/σ	0.06	0.00	0.00	0.01	0.00	0.00	0.06
No. of variables	877	244	406	235	251	244	259
Maximum, minimum density in ΔF map close to Ru (e Å^{-3})	1.49, −1.86	1.11, −1.51	0.55, −0.69	0.94, −1.23	0.40, −0.35	1.23, −1.01	1.10, −1.08

Table 10
Carbons and protons assignment for rings of cluster **5**

Ring	Carbon (δ)	Is connected to hydrogen (δ)
A [a]	C(34) 41.93	2.16
		2.18
	C(33) 32.99	1.68
		1.71
	C(32) 25.01	1.84
		1.80
	C(31) 28.29	1.56
		1.74
	C(30) 22.33	1.74
		1.81
	C(29) 27.25	1.75
		1.58
	C(28) 23.17	1.83
		1.78
B [b]	C(22) 42.06	3.45
		2.20
	C(21) 33.75	2.50
		1.93
	C(20) 27.89	1.75
		1.50
	C(19) 37.74	2.23
		2.21
	C(18) 27.25	1.82
		1.00
	C(17) 23.17	3.23
		2.90

[a] A: C_8H_{14} [C(27)–C(28)–C(29)–C(30)–C(31)–C(32)–C(33)–C(34)].
[b] B: C_8H_{12} [C(16)–C(17)–C(18)–C(19)–C(20)–C(21)–C(22)–C(23)].

References

[1] F. Muller, D.I.P. Dijkhuis, G. van Koten, K. Vrieze, D. Heijdenrijk, M.A. Rotteveel, C.H. Stam, M.C. Zoutberg, Organometallics 8 (1989) 992.
[2] C.J. Adams, M.I. Bruce, B.W. Skelton, A.H. White, J. Organomet. Chem. 420 (1991) 87.
[3] C.J. Adams, M.I. Bruce, B.W. Skelton, A.H. White, J. Organomet. Chem. 423 (1992) 83.
[4] R.D. Adams, J.T. Tanner, Organometallics 8 (1989) 563.
[5] R.D. Adams, G. Chen, L. Chen, M.P. Pompeo, J. Yin, Organometallics 10 (1991) 2541.
[6] S. Jeannin, Y. Jeannin, C. Rosenberger, Inorg. Chim. Acta 1 (1993) 323.
[7] E. Sappa, O. Gambino, L. Milone, G. Cetini, J. Organomet. Chem. 39 (1972) 169.
[8] E. Sappa, A. Tiripicchio, P. Braunstein, Chem. Rev. 83 (1983) 203.
[9] C.S.W. Lau, W.T. Wong, J. Chem. Soc. Dalton Trans. (1998) 3391.
[10] C.S.W. Lau, W.T. Wong, J. Chem. Soc. Dalton Trans. (1999) 607.
[11] D. Braga, P.J. Dyson, F. Grepioni, B.F.G. Johnson, Chem. Rev. 94 (1994) 1585.
[12] A.J. Deeming, in: B.F.G. Johnson (Ed.), Transition Metal Clusters, Wiley, New York, 1980.
[13] (a) G.A. Somorjai, in: L.L. Hegedus (Ed.), Catalyst Design — Progress and Perspectives, Wiley, New York, 1980. (b) G.A. Somorjai, Introduction to Surface Chemistry and Catalysis, Wiley, New York, 1994.
[14] M.J. Hosstetler, L.H. Dubois, R.G. Nuzzo, G.S. Girolami, J. Chem. Soc. Dalton Trans. (1994) 1105.
[15] D. Braga, P.J. Dyson, F. Grepioni, B.F.G. Johnson, C.M. Martin, L. Scaccianoce, A. Steiner, Chem. Commun. (Cambridge) (1997) 1259.
[16] (a) S.L. Ingham, B.F.G. Johnson, C.M. Martin, D. Parker, J. Chem. Soc. Chem. Commun. (1995) 159. (b) D. Braga, F. Grepioni, D.B. Brown, B.F.G. Johnson, M.J. Calhorda, Organometallics 15 (1996) 5723. (c) D. Braga, F. Grepioni, D.B. Brown, B.F.G. Johnson, M.J. Calhorda, L.F. Veiros, J. Chem. Soc. Dalton Trans. (1997) 547.
[17] B.F.G. Johnson, J.M. Matters, P.E. Gaede, S.L. Ingham, N. Choi, M. McPartlin, M.A. Pearsall, J. Chem. Soc. Dalton Trans. (1997) 3251.
[18] A.J. Blake, J.L. Haggitt, B.F.G. Johnson, S. Parsons, J. Chem. Soc. Dalton Trans. (1997) 991.
[19] P.J. Bailey, M.J. Duer, B.F.G. Johnson, J. Lewis, G. Conole, M. McPartlin, H.R. Powell, C.E. Anson, J. Organomet. Chem. 383 (1990) 441.
[20] P.J. Dyson, B.F.G. Johnson, D. Reed, D. Braga, F. Grepioni, E. Parisini, J. Chem. Soc. Dalton Trans. (1993) 2817.
[21] V.G. Albano, M. Sansoni, P. Chini, S. Martinengo, J. Chem. Soc. Dalton Trans. (1973) 651.
[22] C.R. Eady, B.F.G. Johnson, J. Lewis, J. Chem. Soc. Dalton Trans. (1975) 2606.
[23] R.D. Adams, P. Mathur, B.E. Segmüller, Organometallics 2 (1983) 1258.
[24] D. Braga, F. Grepioni, P.J. Dyson, B.F.G. Johnson, P. Frediani, M. Bianchi, F. Piacenti, J. Chem. Soc. Dalton Trans. (1992) 2565.
[25] L.J. Farrugia, Acta Crystallogr. C44 (1988) 997.
[26] C.J. Adams, M.I. Bruce, B.W. Skelton, A.H. White, Chem. Commun. (Cambridge) (1996) 2663.
[27] (a) R.D. Adams, G. Chen, S. Sun, T.A. Wolfe, J. Am. Chem. Soc. 112 (1990) 868. (b) S.-H. Han, S.T. Nguyen, G.L. Geoffroy, Organometallics 7 (1988) 2034. (c) R.D. Adams, J.E. Babin, M. Tasi, Inorg. Chem. 26 (1987) 2561.
[28] L. Braunschweiler, R.R. Ernst, J. Magn. Reson. 53 (1983) 521.
[29] A. Bax, D.G. Davis, J. Magn. Reson. 65 (1985) 355.
[30] P.F. Jackson, B.F.G. Johnson, J. Lewis, M. McPartlin, W.J.H. Nelson, J. Chem. Soc. Chem. Commun. (1980) 1190.
[31] R.D. Adams, W. Wu, Organometallics 12 (1993) 1243.
[32] S.R. Drake, B.F.G. Johnson, J. Lewis, G. Conole, M. McPartlin, J. Chem. Soc. Dalton Trans. (1990) 995.
[33] D.B. Brown, B.F.G. Johnson, C.M. Martin, S. Parsons, J. Organomet. Chem. 536 (1997) 285.
[34] N. Lugan, J.J. Bonnet, S. Rivomanana, G. Lavigne, Organometallics 10 (1991) 2285.
[35] N. Lugan, J.J. Bonnet, S. Rivomanana, G. Lavigne, R. Yanez, R. Mathieu, J. Am. Chem. Soc. 111 (1989) 8959.
[36] A.J. Blake, P.J. Dyson, B.F.G. Johnson, C.M. Martin, J.G.M. Nairn, E. Parisini, J. Lewis, J. Chem. Soc. Dalton Trans. (1993) 981.
[37] D.T. Cromer, J.T. Waber, International Tables for X-Ray Crystallography, vol 4, Kynoch, Birmingham, 1974. (a) Table 2.2B. (b) Table 2.3.1.
[38] G.M. Sheldrick, SHELXS 86, Program for crystal structure solution, Acta Crystallogr. Sect. A. 46 (1990) 467.
[39] SIR 88, M.C. Burla, M. Camalli, G. Cascarano, C. Giacovazzo, G. Polidori, R. Spagna, D. Viterbo, J. Appl. Crystallogr. 22 (1989) 389.
[40] TEXSAN, Crystal structure analysis package, Molecular Structure Corporation, Houston, TX, 1985.